

University of Nebraska - Lincoln
DigitalCommons@University of Nebraska - Lincoln

Architectural Engineering -- Faculty Publications

Architectural Engineering

2012

Effects of inclusion shapes within rigid porous materials on acoustic performance


Hyun Hong

University of Nebraska-Lincoln, icarus1021@gmail.com

Siu-Kit Lau

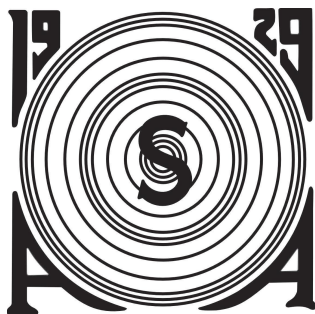
University of Nebraska-Lincoln

Follow this and additional works at: <http://digitalcommons.unl.edu/archengfacpub>

 Part of the [Architectural Engineering Commons](#), [Construction Engineering Commons](#), [Environmental Design Commons](#), and the [Other Engineering Commons](#)

Hong, Hyun and Lau, Siu-Kit, "Effects of inclusion shapes within rigid porous materials on acoustic performance" (2012).
Architectural Engineering -- Faculty Publications. 99.
<http://digitalcommons.unl.edu/archengfacpub/99>

This Article is brought to you for free and open access by the Architectural Engineering at DigitalCommons@University of Nebraska - Lincoln. It has been accepted for inclusion in Architectural Engineering -- Faculty Publications by an authorized administrator of DigitalCommons@University of Nebraska - Lincoln.



**164th Meeting of the Acoustical Society of America
Kansas City, Missouri
22 - 26 October 2012**

Session 1pNS: Noise

1pNS12. Effects of inclusion shapes within rigid porous materials on acoustic performance

Hyun Hong* and Siu-Kit Lau

*Corresponding author's address: Durham School of Architectural Engineering and Construction, University of Nebraska-Lincoln, Omaha, NE 68182-0816, hhong@huskers.unl.edu

The present study investigates the influence of various shapes of inclusions having same volume embedded in a porous rigid material. Previous studies showed improvement of the broadband sound absorption with particular shapes of inclusions. However, different volumes of the inclusions have been considered; therefore, the bulk densities are not the same for comparison. The present study extends the investigations of inclusions in porous materials with same volume (or bulk density) to eliminate the influence by the change of bulk density. The effects of shape will be discussed. Finite element modeling will be used for this study. Total four different shapes: circle, square, ellipse, and triangle, have been studied at various orientations. It has been found that specific configurations can be able to improve the broadband sound absorption compared with reference (no inclusion). It is being expected that a better control of sound absorption of porous materials at desired frequency range can be achieved with the results of the present study.

Published by the Acoustical Society of America through the American Institute of Physics

I. Introduction

Understanding sound propagation in materials is an important aspect in the design of wide range of sound absorbers and insulations. Porous material is commonly used in noise control because of high sound absorption at middle and high frequencies. However, it has a lack of sound absorption at low frequencies, and this lack becomes significant when the thickness of material is less than the quarter wave length of the forcing frequency. In most of the applications, there is a practical limitation using bulky materials. In order to improve sound absorption at low frequencies with thinner materials, two approaches have so far been studied: they are multilayer materials¹⁻⁵ and embedding inclusions⁶⁻⁸. Using multilayer materials can provide better sound absorption without increase of the thickness¹. However, the manufacturing process of multilayer materials is complicated. Another approach is to embed inclusions into the porous material to get additional absorption by scattering and dissipation of sound in the materials⁶. Since the sound absorptions of a porous material with inclusions are varied with the shapes of inclusions^{6,8}, it is worthwhile to investigate the effects of the inclusion shapes on the sound absorptions and thus the optimal inclusion shape for noise control.

There are some existing publications which have addressed the effects of inclusions on control of sound absorptions. Groby et al.⁶ has studied the effects of sizes of circular periodic inclusions and the angle of incident wave. In this research, they found that the sound absorption increases at some frequencies but also reduce sound absorption at the rest of frequencies significantly as the size of inclusion increases. Their results have shown the effect of the size of inclusions; however, the effects of inclusion shapes have not addressed. Nennig et al.⁸ has widely studied rigid or soft inclusions embedded in the materials of different periods of cells and heights at various incident angles. This study found that open shape inclusions (e.g. U-shape) have better broadband absorption, because less porous material is removed from the layer. For the study of U-shape inclusions, it shows good improvement of absorption at over wide range of frequencies which can be explained by the existence of two trapped modes⁹ in the porous layer¹⁰. However, this study did not maintain the same cross-sectional area of the inclusions, so it is unsure whether inclusion shape is the only cause of the change in sound absorption.

In the present study, the effects of various inclusion shapes embedded into porous materials are numerically investigated. Peak absorption coefficient occurs at frequencies close to or below the quarter-wavelength resonant frequency with a hard-backed porous sheet. These peaks are associated with fundamental modes of the porous layer and with the trapped modes related to inclusions.

II. FORMULATION OF THE PROBLEM

A. Description of the configuration

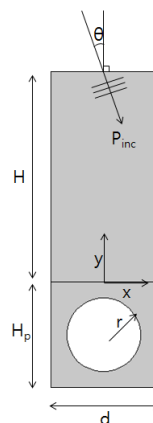


Figure 1. Geometry of the periodic cell

Consider a periodic cell in 2-D consisting of two domains, air and porous materials as shown in Fig.1. The width W and height H_p of porous material are both 0.02m. The height of air domain H is 0.04m. Finite element computation is applied to solve the harmonic wave equation

$$\nabla^2 p + k^2 p = 0, \tag{1}$$

where p and k are acoustic pressure and wave number of sound, respectively. The bottom of the cell and the boundary of inclusion are acoustically rigid; therefore, the normal pressure gradient vanishes and the boundary condition is

$$\left. \frac{\partial p}{\partial n} \right|_{wall} = 0, \tag{2}$$

where n is the outward unit normal to the boundary.

The acoustic plane wave is incident at an oblique angle on the top of the porous cell. This incident wave is expressed by $p_{inc} = Ae^{-i(k_x x + k_y y)}$. We assume that the cell is periodic in the direction x and spatial period is d of 0.02m (see Fig. 1). The side walls of the model satisfy Floquet relation

$$p(x + d, y) = p(x, y)e^{ik_x d}. \tag{3}$$

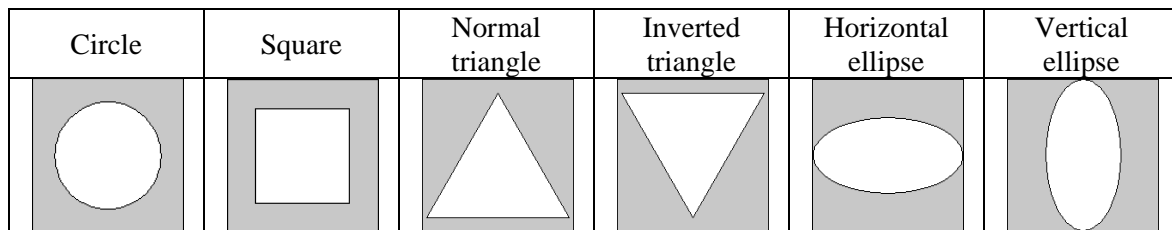


Figure 2. Different shapes of inclusions with inclusion that is 39% of the unit cell (circle, square, normal and inverted triangles, and horizontal and vertical ellipses)

There are six different shapes [i.e., circle, square, triangle (normal, inverted) and ellipse (vertical, horizontal)] of inclusions as shown in Fig. 2. In each case, the inclusion keeps the same area and dimension which is a function of the radius r of the circular inclusion. Therefore, the length side l_{sq} of the square is set equal to $l_{sq} = r\sqrt{\pi}$. The length side l_{tr} of the triangle is set equal to $l_{tr} = r\sqrt{\frac{4}{\sqrt{3}}\pi}$. The ellipse with semi-major axes $l_{el} = r\sqrt{2}$ and semi-minor axes equal $l_{el}/2$. These inclusions were placed at the center of the unit cell. Radius r of 1, 3, 5, and 7mm were evaluated in the present study. Corresponding inclusion areas are 1, 7, 20, and 39% of the unit cell (Area = 0.02m x 0.02m). Incident angles of the excitation plane wave at 0, 30, 45 and 60 degrees has been investigated with the four different sizes and six different shapes of inclusions.

For the incident plane wave, the conservation of energy relation satisfies $Power_{absorp} = Power_i - Power_r$, where $Power_{absorp}$ is absorbed acoustic power, $Power_i$ is incident acoustic power and $Power_r$ is reflected acoustic power. This yields the normal absorption coefficient as

$$\alpha = \frac{Power_{absorp}}{Power_i} = 1 - R = 1 - \frac{I_y - I_i}{I_i}, \tag{4}$$

where I_i is given by $\frac{1[Pa]}{\rho_f c} \cos \theta$, ρ_f is density of air, c is speed of sound in air and θ is incident angle. I_y is y-directional intensity and I_i is y-directional component of incident intensity. I_y is measured at the surface of the porous material.

Numerical calculations by finite element method (FEM) have been performed within the frequency range from 20 Hz to 9,000 Hz. For all calculations, the ambient and saturating fluid is air

($c = \sqrt{\gamma P_0 / \rho_f}$ with air density $\rho_f = 1.213 \text{ kg/m}^3$, atmospheric pressure $P_0 = 1.01325 \times 10^5 \text{ Pa}$, heat capacity $\gamma = 1.4$, and air viscosity $\eta = 1.839 \times 10^{-5} \text{ kg/m}^3$). The maximum element size of the simulation is $\lambda_{\min}/15$, where λ_{\min} is c/f_{\max} . f_{\max} is the maximum studied frequency at 9,000 Hz. The mesh method is triangular mesh in all domains.

B. Material modeling

Rigid frame porous material is modeled using the Johnson-Champoux-Allard-Lafarge model. The dynamic compressibility χ and dynamic density ρ are

$$\chi = \frac{1}{K} = \frac{1}{\gamma P_0} \left[\gamma - (\gamma - 1) \left(1 + \frac{\eta \Phi}{i \omega q'_0 \rho_f} \sqrt{1 + \left(\frac{2q'_0}{\Phi \Lambda'} \right)^2 \frac{i \omega \rho_f \text{Pr}}{\eta}} \right)^{-1} \right], \quad (5)$$

$$\rho = \frac{\rho_f \alpha_\infty}{\Phi} - \frac{i \eta_c}{\omega q_0}, \quad (6)$$

where K is the bulk modulus, γ is the specific heat ratio, P_0 is the atmospheric pressure, η is the viscosity, Φ is the porosity, q'_0 is the thermal permeability, ρ_f is the density of the fluid in the pores, Pr is the Prandtl number, Λ' is the thermal characteristic length, α_∞ is the tortuosity, and σ is the static air flow resistivity¹¹. The complex frequency-dependent viscosity η_c is given as

$$\eta_c = \eta \sqrt{1 + \left(\frac{2\alpha_\infty q_0}{\Phi \Lambda} \right)^2 \frac{i \omega \rho_f}{\eta}}, \quad (7)$$

where Λ is the viscous characteristic length. The static thermal resistivity $\sigma' = 8\alpha_\infty \eta / \Phi \Lambda^2$.¹²

Table I. Parameters of the porous foam. With the porosity Φ , flow resistivity σ , the tortuosity α_∞ , and the viscous and thermal characteristic length Λ and Λ'

Material	Φ	σ [Nm^{-4}s]	α_∞	Λ [μm]	Λ' [μm]	Reference
Fireflex	0.95	8,900	1.42	180	360	6

In this study, we consider rigid inclusions embedded in Fireflex, and the physical properties are shown in Table I.

III. RESULTS AND DISCUSSION

The absorptions of the porous layer embedded by inclusions are numerically analyzed. The commercial software of COMSOL Multiphysics was used for FEM simulation. Results will be discussed in three aspects: shapes, sizes, and incident angles.

A. Effects of inclusion shapes

Variation of the absorption coefficients with different inclusion shapes and the normal incident wave are presented in this part. Inclusion size is kept at 20% of the unit cell of porous material.

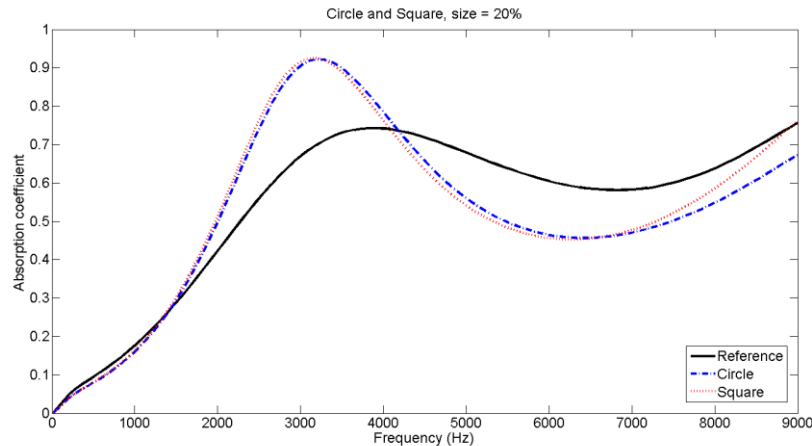


Figure 3 Absorption coefficient of a $H_p = 2\text{cm}$ thick porous sheet of Fireflex backed by a rigid flat plate (—) without inclusion, (— · — · —) with circular inclusions and (- - -) with square inclusions under normal incident wave.

The absorption coefficients with foam plate without inclusion, with circular inclusions and with square inclusions are compared in Fig. 3. The results of 20% size circular inclusion are shown. The porous material with circular inclusions has increased sound absorption between 1,410Hz and 4,180Hz and decreased absorption at other frequency being studies compared with the reference (without inclusions). The peak absorption coefficient at around f_{cp} (resonant frequency with circular inclusion) = 3195 Hz can be explained by trapped modes⁸. This mode is the perturbation which makes sound energy decay and absorb more in the porous materials.

The porous layer with square inclusions has increased sound absorption from 1,322Hz and 4,082Hz and decreased absorption below 1,322Hz. Both circular inclusions and square inclusions show similar changes of absorption coefficients below 6,600Hz. The frequency of the peak absorption coefficient with square inclusion f_{sp} is very close to the frequency at peak absorption coefficient with circular inclusion f_{cp} . This may be explained by the symmetry of both inclusions. Technically both inclusions have different shapes; however, both configurations are symmetric to the horizontal line passing the center of the inclusions and to the vertical line between inclusions. One may notice that we can get increased absorption from specific range of frequencies, but may also have decreased absorption at other frequencies with both circular and square inclusions.

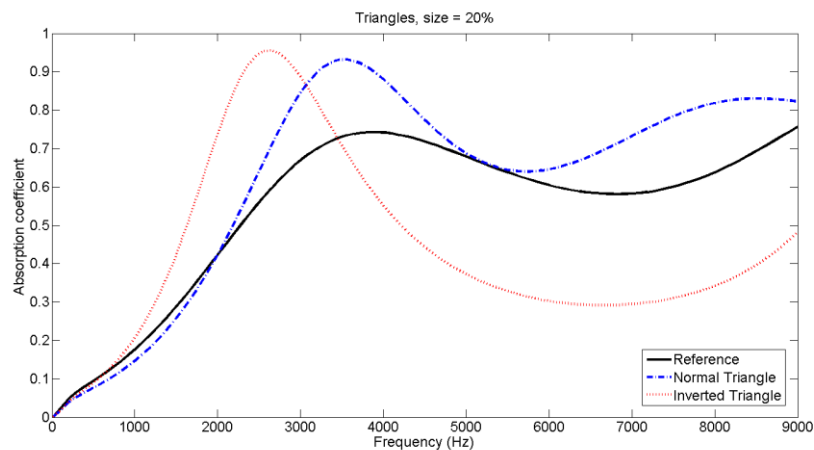


Figure 4 Absorption coefficient of a $H_p = 2\text{cm}$ thick porous sheet of Fireflex backed by a rigid flat plate (—) without inclusion, (— · — ·) with normal triangular inclusions and (- - -) with inverted triangular inclusions under normal incident wave.

The absorption coefficients with a 2cm-thick foam plate without inclusion, with normal triangular inclusions and with inverted triangular inclusions are compared as shown in Fig. 4. Equilateral triangles have been considered. Similar to circular and square inclusions, both normal and inverted triangular inclusions in Fireflex result in increased and decreased sound absorptions at different frequencies. As shown in Fig. 4, inverted triangular inclusion increases sound absorption coefficients at 636Hz to 3,447Hz, and significantly decreases sound absorption at above 3,447Hz compared with the reference materials. There are a peak absorption coefficient at $f_{itp} = 2651$ Hz and the dip at $f_{itd} = 6642$ Hz. Normal triangular inclusions offer increase of sound absorption coefficients at frequencies above around 2000 Hz and a slight reduction at frequencies below around 2000 Hz.

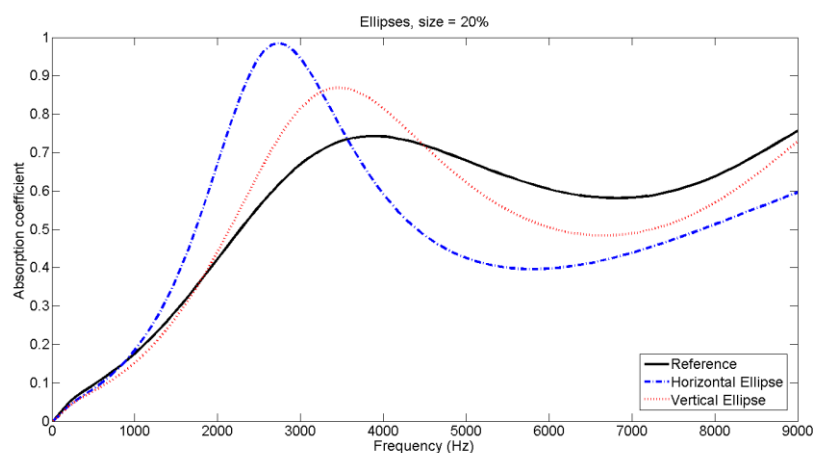


Figure 5 Absorption coefficient of a porous sheet ($H_p = 2\text{cm}$ thick) of Fireflex backed by a rigid flat plate (—) without inclusion, (— · — ·) with horizontal ellipsoidal inclusions and (- - -) with vertical ellipsoidal inclusions under normal incident wave.

The absorption coefficients with a 2cm-thick foam plate without inclusion, with horizontal ellipsoidal inclusions and with vertical ellipsoidal inclusions are compared as shown in Fig. 5. The ratio of a semi-minor axis to a semi-major axis is 1/2. The porous sheet with horizontal ellipsoidal inclusions has increased absorption between 870Hz to 3,565Hz and peak absorption coefficient occurs at $f_{hep} = 2,741\text{Hz}$ as shown in Fig. 5. Decreased absorption above 3,565 Hz, and the dip at $f_{hed} = 5825$ Hz have been observed. The porous sheet with vertical ellipsoidal inclusions has increased absorption between 1798 Hz and 4484 Hz. Also, decreased absorption below 1798 Hz and above 4484 Hz are observed. The peak absorption coefficient is at $f_{vep} = 3467$ Hz, and the dip is at $f_{ved} = 6642$ Hz.

B. Effects of inclusion sizes

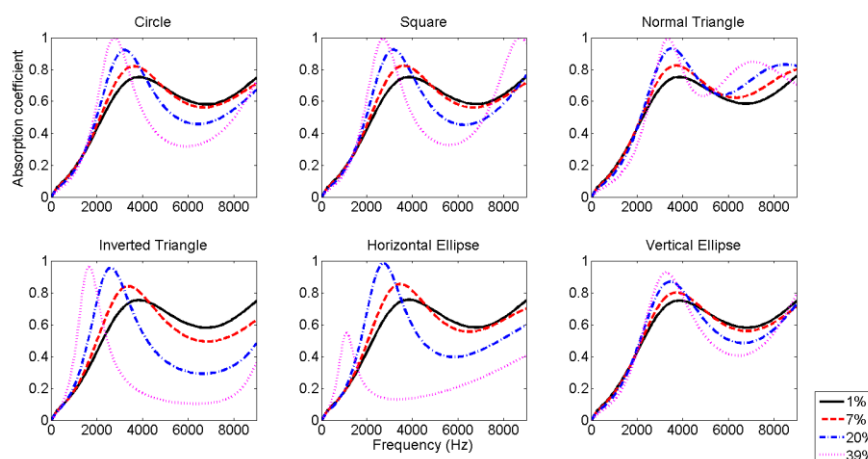


Figure 6 Absorption coefficient of a porous sheet ($H_p = 2\text{cm}$ thick) of Fireflex backed by a rigid flat plate with inclusion size of (—) 1%, (- - -) 7%, (- · - ·) 20% and (· · ·) 39% under normal incident wave.

Effects of size variation of inclusions are shown in this sub-section. Fig. 6 shows sound absorption change by size variation under normal wave incidence. There is a general trend that the peak and dip move to lower frequencies and the width of peaks narrows as the inclusion size increases. The absorption coefficients approach that of the reference as the inclusion size decreases. There is an exception of this trend: for the normal triangular inclusion case, the peak slightly moves to lower frequencies and absorption increases as inclusion size increases. However, the dips of absorption coefficient curves increase slightly as inclusion size increases which is different from the trends of other inclusion shapes. Consequently, it is possible to have increased peak absorption at low frequency band with less absorption loss at high frequency bands. It is also observed that the peak absorption of 39% horizontal ellipsoidal inclusion case is smaller than that of 20% horizontal ellipsoidal inclusion. At first glance, it seems the peak absorption increases as inclusion size increases; however, it starts to decrease after the specific size. This phenomenon has been shown in Ref. 6 with circular inclusion. As inclusion size increases, the peak absorption coefficient moves to lower frequencies, and the peak absorption coefficient generally increases reaching a maximum of unity. However, the peak absorption coefficient will decrease as the inclusion size further increases. There are two possible reasons for this phenomenon as explained in Ref. 6. As the inclusion size increases, these inclusions form a kind of layer of inclusions. The wave is mainly reflected on the inclusions and no longer propagate in the layer towards the rigid backing, or because the bulk density of inclusion becomes insignificant. Based on these observations, we may say that to control the absorption peak and obtain a desired absorption, the inclusion size must be optimized.

C. Effects of incident angles

Different incident angles are depicted with the inclusion size of 20% of the unit porous material (Fig. 7).

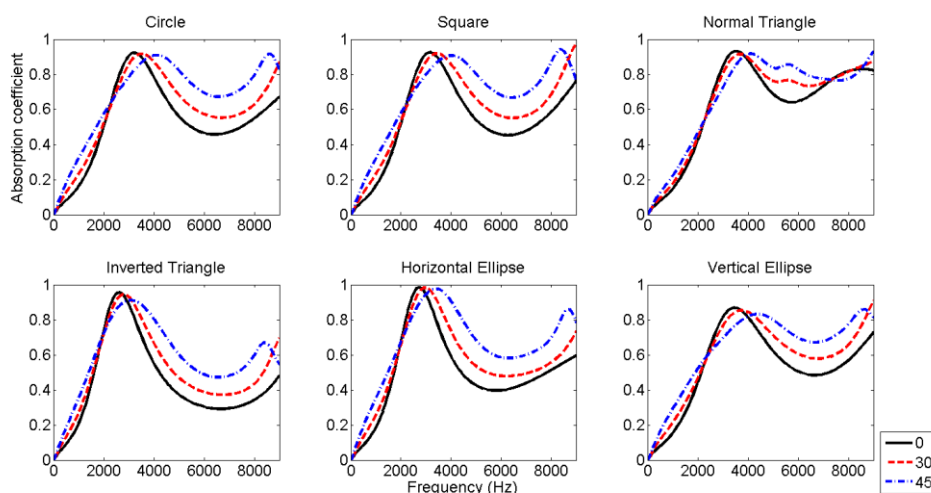


Figure 7 Absorption coefficient of a porous sheet ($H_p = 2\text{cm}$ thick) of Fireflex backed by a rigid flat plate with incident wave angles of (—) 0 degree, (- - -) 30 degree, and (- · - ·) 45 degree with 20% size inclusions.

There is a trend that the peak absorption moves to higher frequencies and absorption below 2,000Hz increases as incident angle increases. Also, the absorption increases between 4,000Hz and 8,000Hz with larger incident angles.

IV. CONCLUSIONS

In this study, the influences of different inclusion shapes embedded in a porous sheet backed by a rigid plate were studied. In total six different shapes were tested with four sizes and four incident angles. It has been shown that using inclusions improves the low frequency absorption but also results in decrease of absorptions at higher frequencies. It has been shown that normal triangle inclusion with specific size is able to provide a better overall absorption compared with the reference (no inclusion). By increasing the inclusion size, we can get the maximum absorption at a certain frequency at the particular size of inclusion. Absorption decreases when the size of inclusion is away from this optimal size. This study shows that it is possible to optimize the inclusion shape while maintaining the same inclusion area to get overall improved sound absorption. Based on this analysis, it is possible to design better sound absorption in porous materials using inclusions, and also to decide whether we use inclusions or not for given situations. Future work is needed to investigate the method of optimization of inclusion shapes to get desired improvement in given conditions.

IV. Acknowledgments

The present work was supported by the Nebraska ESPCoR First award.

REFERENCES

- ¹ J. -F. Allard and N. Attala, *Propagation of sound in porous media: modeling and sound absorbing materials* (John Wiley & Sons, 2009), pp.243-281
- ² J. -F. Allard, Y. Champoux, and C. Depollier, "Modelization of layered sound absorbing materials with transfer matrices," *J. Acoust. Soc. Am.* **82** (5), 1792-1796 (1987)
- ³ B. Brouard, D. Lafarge, J.-F. Allard, "A general method of modeling sound propagation in layered media," *J. Sound Vib.* **183** (1), 129-142 (1995)
- ⁴ W. Lauriks, A. Cops, J. -F. Allard, C. Depollier, and P. Rebillard, "Modelization at oblique incidence of layered porous materials with impervious screens," *J. Acoust. Soc. Am.* **87** (3), 1200-1206 (1989)
- ⁵ P. Rebillard, J. -F. Allard, C. Depollier, and P. Guignouard, "The effect of a porous facing on the impedance and the absorption coefficient of a layer of porous material," *J. Sound Vib.* **156** (3), 541-555 (1992)
- ⁶ J. -P. Groby, O. Dazel, and A. Duclos, "Enhancing the absorption coefficient of a backed rigid frame porous layer by embedding circular periodic inclusions," *J. Acoust. Soc. Am.* **130** (6), 3771-3780 (2011)
- ⁷ E. Gourdon and M. Seppi, "On the use of porous inclusions to improve the acoustical response of porous materials: Analytical model and experimental verification," *Appl. Acoust.* **71**, 283-298 (2010)
- ⁸ B. Nennig, Y. Renou, J. -P. Groby, and Y. Aurégan, "A mode matching approach for modeling two dimensional porous grating with infinitely rigid or soft inclusions," *J. Acoust. Soc. Am.* **131** (5), 3841-3852 (2012)
- ⁹ T. Utsunomiya and R. Eatock Talyor, "Trapped modes around a row of circular cylinders in a channel," *J. Fluid Mech.* **386**, 259-279 (1999)
- ¹⁰ C. Linton and P. McIver, "Embedded trapped modes in water waves and acoustics," *Wave Motion* **45**, 16-29 (2007)
- ¹¹ D. Lafarge, P. Lemarinier, J. -F. Allard, and V. Tarnow, "Dynamic compressibility of air in porous structures at audible frequencies," *J. Acoust. Soc. Am.* **102** (4), 1995-2006 (1997)
- ¹² D. L. Johnson, J. Koplik, and R. Dashen, "Theory of dynamic permeability and tortuosity in fluid-saturated porous media," *J. Fluid Mech.* **176**, 379-402 (1987)